Finite-temperature instabilities of a two-dimensional dipolar Bose gas at arbitrary tilt angle

Pengtao Shen and Khandker F. Quader*
Department of Physics, Kent State University, Kent, Ohio 44242, USA

(Received 7 December 2020; accepted 30 March 2021; published 12 April 2021)

Advances in creating stable dipolar Bose systems and ingenious box traps have generated great interest in the field of cold bosons. Theory study of dipolar bosons at finite temperature T has been limited. We study two-dimensional dipolar bosons at arbitrary tilt angle θ using finite-T random phase approximation. We show that a comprehensive understanding of phases and instabilities at nonzero T can be obtained by concurrently considering dipole strength, density, temperature, and θ. We find the system to be in a homogeneous noncondensed phase that undergoes a collapse transition at large θ, and a finite momentum instability, signaling a striped phase, at large dipolar strength; there are important differences from the $T = 0$ case. As $T \to 0$, a Bose-condensed phase appears at critical dipolar strength, and at critical density. Our predictions for a polar molecule system, ^{41}K ^{87}Rb, and ^{166}Er may provide tests of our results.

DOI: 10.1103/PhysRevA.103.043317

The nature of excitations, phases, and instabilities of interacting Bose systems has been a subject of long-standing interest. The extraordinary development of the field of ultracold atoms, tremendously advanced by novel experimental techniques over the past several years, has led to intense research. In recent years, there has been considerable interest in systems with long-range and anisotropic interactions; examples are bosonic and fermionic atoms, and polar molecules experiencing dipolar interactions.

Recent experimental advances in creating stable dipolar bosonic systems, including polar molecules with large electric dipole moments, have led to vigorous research activities. Dipolar Bose-Einstein condensates (BECs) have been realized in chromium [1] (^{52}Cr), and in lanthanide atoms (such as dysprosium and erbium [2]), which have larger magnetic moments. Recent observation [3] of a roton mode, for the first time, in dipolar ^{166}Er (magnetic moment 7 μ_B) in a cigar-shaped trap geometry constitutes a significant development. The realization of high phase-space density systems of polar molecules, such as ^{87}Rb ^{133}Cs [4,5] and ^{41}K ^{87}Rb [6,7], holds promise for realization of quantum degeneracy and dipolar BECs. In general, the electric dipole moments of the polar molecules are substantially larger than the magnetic dipole moments of atoms; for example, the RbCs system has a sizable electric dipole moment, $\sim$1.28 D. Ingenious box traps constitute another significant development. There have been box-trap experiments on bosons subjected to contact interaction [8–10], while those on dipolar systems are ongoing.

The long-range and anisotropic nature of dipolar interaction, with a region of attraction, can give rise to novel quantum phases, even in dilute systems. A sizable body of theory work, based on Monte Carlo and Bogoliubov–de Gennes (BdG) methods, exists at zero temperature ($T = 0$). The existence of a roton mode and density wave phase has been found in BdG calculations studying the properties of the BEC ground state [11–15]. Solid and stripelike crystal phases have been predicted in Monte Carlo simulations [16,17]. Such a stripe phase of the dipolar Bose system provides a promising candidate [18–22] for an intrinsic supersolid, but the issue of supersolidity in two-dimensional (2D) dipolar bosons has been a subject of debate [23,24].

A purely dipolar 3D system is usually unstable towards collapse due to the attractive component of the interaction. A trap helps to stabilize the system; this depends strongly on trapping geometry [1,25]. In 2D, the stability issue of dipolar bosons may be richer [26,27]. There have been studies [28,29] of density response in 3D and 2D Bose gas with attractive constant interaction, based on random phase approximation (RPA). A similar study of dipolar bosons in a cylindrical trap at finite temperature shows that a pancake geometry trap stabilizes the system [30]. This brings up the question as to whether purely 2D dipolar bosons are stable at finite temperature. Theoretical study of 2D dipolar boson gas at finite temperature has been limited.

In this paper, we present results of our study of a 2D dipolar Bose system at *nonzero temperatures*, using finite-temperature RPA [28,30]. A key point of the paper is that a broad perspective on the phases and instabilities of the system at *finite temperature* can be attained by considering several tunable knobs: density, temperature, interaction strength, and the orientation of dipole moments to an external field, i.e., tilt angle. We construct several informative phase diagrams based on our study of dipolar length (strength) versus dipole tilt angle at a given temperature; RPA critical temperature and critical density versus dipolar length for a given tilt angle, and critical temperature versus critical density for a given tilt angle. In particular, at finite temperature, we find the system to be in a homogeneous noncondensed phase that undergoes a collapse transition at large tilt angles, and a finite momentum instability, signaling a striped phase, at sufficiently large values of dipolar coupling strength. The linear q dependence of the 2D dipolar interaction is manifested in a new density wave instability in a broad regime similar to that in 2D dipolar

*Corresponding author: quader@kent.edu

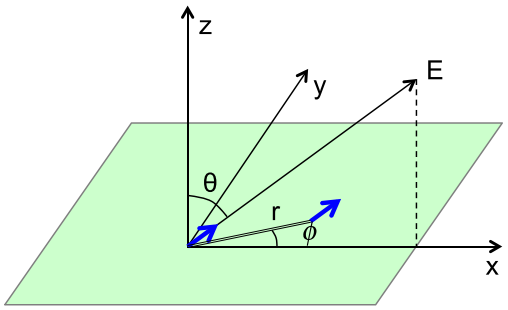

FIG. 1. 2D dipoles in the x-y plane with tilt angle θ that defines the direction of the electric or magnetic field **E** relative to the z direction. ϕ is the angle in the x-y plane, relative to the x direction.

fermions [26,27]. As $T \to 0$, for sufficiently small tilt angles, a BEC appears at a critical dipolar strength, and at a critical density.

While our results should apply generally to 2D dipolar bosons at arbitrary temperature, specific predictions, based on the parameters of the polar molecule system, ^{87}Rb ^{133}Cs, can serve as tests of our results. We briefly discuss the effects of an additional contact interaction. The aforementioned box traps make the study of homogeneous systems directly relevant and testable.

We consider a gas of dipolar bosons of mass m and electric or magnetic dipole moment d. The dipoles are confined to be in the x-y plane, and the dipole moments are aligned by an external electric field **E** or magnetic field **B**, subtending an angle θ with respect to the z axis, as shown in Fig. 1.

To explore the stability of the system, we consider the static density-density correlation function $\chi(q) \equiv \chi(q, w = 0)$, which determines the stability of a system against density fluctuations. When $\chi(q)$ becomes positive at wave vector q, the system has density wave instability and may undergo a transition to the striped phase [26,27]; if it becomes positive as $q \to 0$, the system will develop negative compressibility and collapse.

In standard RPA, the density-density correlation function can be diagrammatically expanded in terms of the bare response function χ_0 (see Appendix A, Fig. 6). For the stability condition against density fluctuations of finite momentum, the direct scattering of particle-hole excitations dominates over the exchange scattering because of the linear momentum dependence of $V_{2D}(q)$ [27,30,31]. So, we neglect the exchange scattering of particle-hole excitations. Also, since in 2D, there is no BEC at finite temperature, there is no contribution from the condensate in the RPA response. Then,

$$\chi(q, \omega) = \frac{\chi_0(q, \omega)}{1 - V(q)\chi_0(q, \omega)}, \tag{1}$$

with

$$\chi_0(q, \omega) = \int \frac{d\mathbf{k}}{(2\pi)^d} \frac{f(k - q/2) - f(k + q/2)}{\hbar\omega - \left(\varepsilon_{k+q/2} - \varepsilon_{k-q/2}\right)}, \tag{2}$$

where $\varepsilon_k = \hbar^2 k^2/2m$ is the free particle kinetic energy and $f(q)$ is the Bose distribution function with chemical potential μ. For noninteracting bosons, $\chi = \chi_0$ and is always negative, so the system is stable. For interaction with an attractive channel, the system can become unstable depending on the interaction.

To proceed, we first need to evaluate the finite-temperature bare response function, Eq. (2). The asymptotic behavior is given by the following (for details, see Appendix B).

In the $q\lambda_T \ll 1$ region,

$$\chi_0(q, T) = -\frac{m}{2\pi\hbar^2} \frac{1}{e^{-\beta\mu} - 1}[1 + O(q\lambda_T)^2], \tag{3}$$

where $\lambda_T = \sqrt{2\pi\hbar^2\beta/m}$ is the thermal de Broglie wavelength and $\beta = 1/k_B T$.

In the $q\lambda_T \gg 1$ region, the behavior is temperature independent, and

$$\chi_0(q) = -\frac{4nm}{\hbar^2 q^2}. \tag{4}$$

In calculating RPA responses, we take the bare response function to be that of a noninteracting system and use the noninteracting gas to calculate the chemical potential $\mu(T, n)$. For an ideal two-dimensional boson gas, the density is

$$\begin{aligned} n &= \int \frac{d\mathbf{k}}{(2\pi)^2} \frac{1}{e^{\beta(\varepsilon_k - \mu)} - 1} \\ &= \lambda_T^{-2} g_1(e^{\beta\mu}), \end{aligned} \tag{5}$$

where $g_v(z) = \sum_j z^j/j^v$ is the polylogarithm function. The chemical potential μ is

$$\mu = \frac{1}{\beta} \ln\left[1 - \exp\left(-n\lambda_T^2\right)\right]. \tag{6}$$

As the temperature decreases, $\chi_0(q)$ increases. In the classical limit, $\beta\mu \gg -1$, Eq. (3) becomes $\chi_0(0) = -n/T$, independent of Bose statistics. In the quantum limit, $\beta\mu \ll -1$, Eq. (3) becomes $\chi_0(0) = -\frac{m}{2\pi\hbar^2} e^{n\lambda_T^2}$. Since there is no upper limit for $g_1(z)$ at zero chemical potential, there is no BEC in 2D at finite temperature. In the limit of zero temperature, $\lim_{T\to 0} \mu = 0$, and $\lim_{T\to 0} n(k) = n\,\delta(k)$. The limiting behavior at zero temperature is the BEC state; Eq. (3) becomes $\chi_0(0, 0) = -\infty$, and Eq. (4) becomes the response function of ideal bosons for all momenta at $T = 0$. Thus at $T = 0$, the finite-T RPA can be shown to be equivalent to BdG theory [32].

It is convenient to look at the inverse of static density-density correlation function $\chi(\mathbf{q})$, given by

$$\frac{1}{\chi(\mathbf{q})} = \frac{1}{\chi_0(q)} - V(\mathbf{q}), \tag{7}$$

where $V(\mathbf{q})$ is the dipole-dipole interaction (DDI), given by $V(\mathbf{q}) = V_s + V_l(\mathbf{q})$, with

$$\begin{aligned} V_s &= 2\pi d^2 \frac{P_2(\cos\theta)}{r_c}, \\ V_l(\mathbf{q}) &= -2\pi d^2 q(\cos^2\theta - \sin^2\theta\cos^2\phi), \end{aligned} \tag{8}$$

where r_c is a short-range cutoff [33]. In quasi-2D geometry, it depends on the trapping size in the z direction [11]. The first term, V_s, is momentum independent and acts like a short-range interaction. The second term depends linearly on the magnitude of momentum. In the y direction ($\phi = \pi/2$), the interaction is the most attractive; therefore the instability

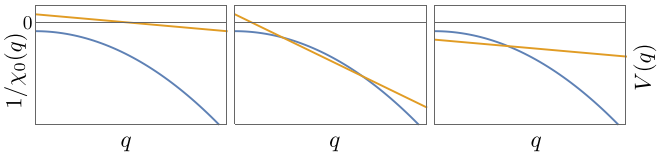

FIG. 2. Schematic illustration of the three cases of response function discussed in the text. The curve is $1/\chi_0(q)$, and the line is $V(q)$.

occurs at momenta in the y direction. Three distinct cases may be noted:

(1) $1/\chi_0(q) - V(q) < 0$ everywhere: The system is in uniform normal stable phase.

(2) $1/\chi_0(q) - V(q) > 0$ at finite q: The system undergoes density wave instability and has striped phase.

(3) $1/\chi_0(q) - V(q) > 0$ at $q = 0$: The system has negative compressibility and collapses.

Figure 2 shows schematically the behavior of $1/\chi_0(q)$ and $V(q)$ for the three cases. $1/\chi_0(q)$ is approximately quadratic in q with intercept $1/\chi_0(0) \leqslant 0$; $V(q)$ is linear in q with negative slope and positive or negative intercept depending on the tilt angle. Note that an instability at finite q is possible for a dipolar system in 2D, but not in 3D [30]. This is because $V(q)$ is independent of the magnitude of momentum in 3D [26].

The behavior of the response function for the 2D dipolar Bose gas at nonzero T can be generally categorized into two regimes with respect to tilt angle θ:

(a) $\theta < \cos^{-1}\frac{1}{\sqrt{3}}$: The short-range interaction $V(q=0)$ is positive, and $1/\chi_0(0) \leqslant 0$. Then, $1/\chi_0(0) - V(0) \leqslant 0$ is always satisfied, and thus it is impossible for the system to collapse. However, the instability condition could be satisfied at finite q_y with a sufficiently strong dipole interaction strength, describable by dipolar length, $a_{dd} = md^2/\hbar^2$. Thus the system is unstable against a density fluctuation with wave vector q_y. This indicates a transition from the normal phase to a striped phase.

(b) $\theta > \cos^{-1}\frac{1}{\sqrt{3}}$: In this region, the short-range interaction becomes negative. At zero temperature, the bare response function diverges at $q = 0$ and $1/\chi_0(0) = 0$, so the system cannot support any attractive short-range interaction. Thus it always collapses at $T = 0$, as in the BdG approach. However, *at finite temperature*, the bare response function has a nonzero negative value at $q = 0$. As a result, it can support attractive short-range interaction that is sufficiently small. The system first undergoes a transition from normal phase to a striped phase and then collapses as a_{dd} increases further. At large tilt angles close to $\pi/2$, the long-range interaction becomes zero, and the total interaction is dominated by the negative short-range part of the dipolar interaction. Then the system goes from the normal to the collapse phase without going through an intermediate striped phase.

For a fixed density and temperature, the dipole interaction strength a_{dd} can be changed via the strength of the external field, and the dipolar tilt angle θ can be changed by varying the direction of external field. In Fig. 3, we show the calculated stability diagram for critical dipole interaction strength a_{dd} versus the tilt angle θ for the polar molecule, ^{87}Rb ^{133}Cs, at $T = 0$ and $T = 20$ nK. We have chosen the density to be

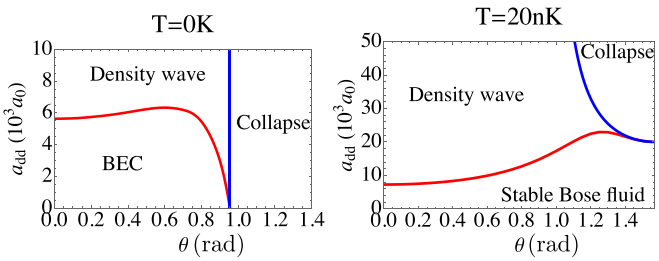

FIG. 3. Critical dipole interaction strength a_{dd} vs tilt angle θ for a system of polar molecule ^{87}Rb ^{133}Cs at $T = 0$ and $T = 20$ nK. a_{dd} is in units of the Bohr radius a_0. Red and blue curves are lines of density wave and collapse instabilities, respectively.

$n = 10^{12}$ m^{-2}, the cutoff to be $r_c = 10^4$ a_0, and the mass of ^{87}Rb ^{133}Cs to be $m = 220$ u (unified atomic mass unit). At $T = 0$ K, for $\theta < 0.955$, the system goes from a stable BEC phase to a density wave instability, as dipole strength a_{dd} increases. The system collapses for any dipole strength when $\theta > 0.955$. On the other hand, at $T = 20$ nK, a density wave instability appears as a_{dd} increases, even for tilt angle $\theta > 0.955$. The system eventually collapses as θ is increased further. That the collapse occurs at a larger value of θ_c compared with that in the $T = 0$ case may be understood on noting the interplay between the DDI and the bare T-dependent response, $1/\chi_0(T)$, in the RPA response function.

A study of critical temperature T_c and critical density n_c, albeit within the RPA, provides another perspective on phases and density wave instability in the system. We first calculate T_c and critical density n_c, each as a function of a_{dd}, for a fixed tilt angle θ. Figure 4 shows our results for the physical system ^{87}Rb ^{133}Cs for $\theta = 0$ and 0.4. T_c and n_c are calculated using the condition $1/\chi(q, T, n) = 0$. For calculation of T_c, we choose the system density to be 10^{12} m^{-2}, and for n_c, we choose the system temperature to be 10 nK. In the context of density wave instability, a key point here is that the critical temperature and critical density behave opposite to each other with increasing dipole strength; that is, T_c increases and n_c decreases when dipole strength is increased (see Fig. 4). The terminating point ($T = 0$) of the T_c curves signifies the onset a_{dd} for BEC; this is dependent on the tilt angle.

Next, we construct temperature-density (T-n) stability diagrams for fixed dipole strengths a_{dd} and tilt angles θ. For $\theta < \cos^{-1}\frac{1}{\sqrt{3}}$, as temperature decreases and density increases, the system goes through a transition from stable Bose fluid phase to a density wave (DW) phase. At $T = 0$, there is a

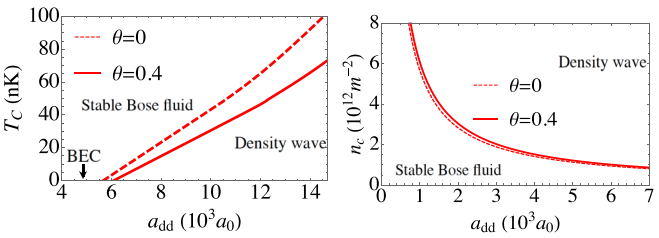

FIG. 4. Critical temperature and critical density for density wave instability of ^{87}Rb ^{133}Cs at tilt angles $\theta = 0$ and 0.4. Left: T_c vs a_{dd}, for $n = 10^{12}$ m^{-2}. Right: n_c vs a_{dd} at $T = 10$ nK.

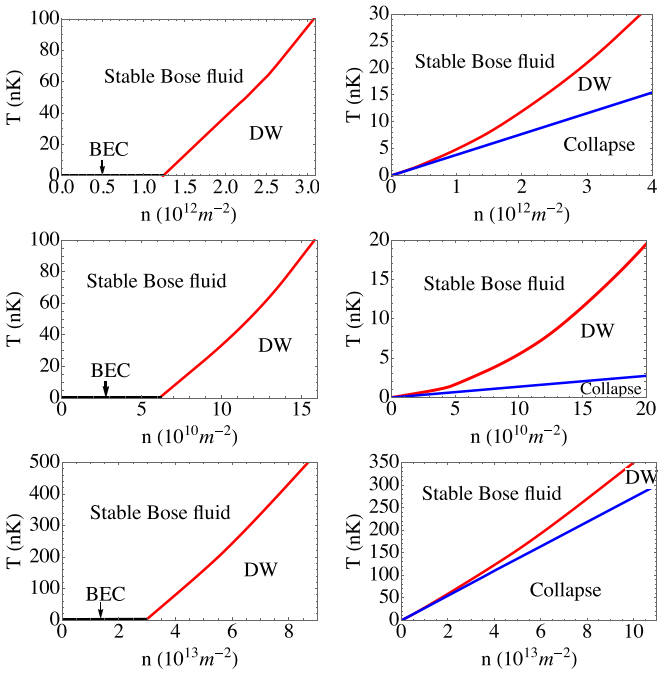

FIG. 5. Calculated T-n stability diagrams for dipolar Bose gas at $\theta = 0$ (left column) and $\theta = 1$ (right column). The top row is for ^{41}Rb ^{87}Cs with dipole moment $d = 0.355$ D; the middle row is for ^{41}Rb ^{87}Cs with $d = 1.22$ D; and the bottom row is for ^{166}Er with $d = 7\ \mu_B$. The red curves denote lines of density wave instability which occur at low temperature and high density for $\theta = 0$. For $\theta = 1$, the system goes from a stable Bose fluid phase to density wave instability, and then to a collapse phase (blue line) as temperature decreases and density increases.

critical density below which there is no density wave instability, and the system is a BEC. For $\theta > \cos^{-1}\frac{1}{\sqrt{3}}$, as temperature decreases and density increases, the system goes through a transition from stable Bose fluid to a density wave phase to a collapse phase. In Fig. 5, we show the calculated T-n stability diagrams, for $\theta = 0$ and $\theta = 1$, using parameters relevant to several physically realized dipolar boson systems, namely, the polar molecule ^{87}Rb ^{133}Cs with electric dipole moment of 0.355 D and $a_{dd} = 4586\ a_0$ (accessible in experiment) [4]; ^{87}Rb ^{133}Cs with electric dipole moment of 1.22 D and $a_{dd} = 93\,084\ a_0$ (the maximum value possible in experiments); and ^{166}Er with magnetic dipole moment of $7\ \mu_B$ and $a_{dd} = 196\ a_0$ [3]. The sets of plots show that for larger dipolar interaction strengths a_{dd}, the instability occurs at a larger density and lower temperature; compare, for example, the plots for ^{87}Rb ^{133}Cs with electric dipole moment of 1.22 D ($a_{dd} = 93\,084\ a_0$) with the plots for ^{166}Er with magnetic dipole moment of $7\ \mu_B$ ($a_{dd} = 196\ a_0$). Density wave instability occurs at low temperature and high density for small tilt angle. For large tilt angle, the system goes from stable Bose fluid phase to density wave instability and then to collapse as temperature decreases and density increases; no discernible region of BEC appears at $T = 0$ (as seen for $\theta = 1$).

We have considered the effect of an additional short-range interaction g, originating from van der Waals interaction between atoms or molecules; this results in total interaction $V(q) = g + V_{\rm dipole}(q)$. Within the RPA, the main modifications are as follows: a repulsive g increases the critical tilt angle θ_c to a value larger than 0.955, while an *attractive* g decreases it. This is because θ_c is now determined by the net short-range interaction, which has contribution from the contact interaction, in addition to that contained in the dipole interaction. Adding a repulsive g increases the critical a_{dd} for instability, while an attractive g decreases this (see Appendix C, Fig. 8).

We have shown that a broad understanding of the nature of phases and instabilities in a 2D dipolar Bose gas at finite temperature may be obtained by concurrently exploring tunable system parameters, namely, density, temperature, interaction strength, and tilt angle. The presented stability diagrams provide different perspectives on the nature of the instabilities. We have used a finite-temperature version of the RPA, the RPA being a well-established many-body method that has proved to be useful in describing collective modes and instabilities in quantum fluids. At $T = 0$, our finite-temperature RPA reproduces the BdG results, as expected [32]; for example, a density wave instability occurs at the critical dipolar strength and critical density that is consistent with that found in zero-T BdG calculation. Our approach and results should not only be of interest within the field of cold bosons but also appeal to a broader audience interested in phase and instabilities of Bose systems generally, and also systems with long-range and anisotropic interactions. Our results may be compared with previous work in 3D with attractive contact interaction [28], or dipolar interaction [30], wherein possible long-wavelength ($q \to 0$) instabilities were studied. We note that a density wave instability usually triggers a long-range order of the stripe phase. At finite temperature, enhanced fluctuation in 2D will destroy the long-range order, but a quasi-long-range order may survive. A phase transition belonging to the usual Berezinskii-Kosterlitz-Thouless universality class is expected; this has been studied in Monte Carlo simulations [34,35]. Thus the T_c curves discussed here are, in a strict sense, RPA instability lines. Accordingly, our T-n phase diagram may need to be modified at low temperature; this is beyond the scope of the RPA.

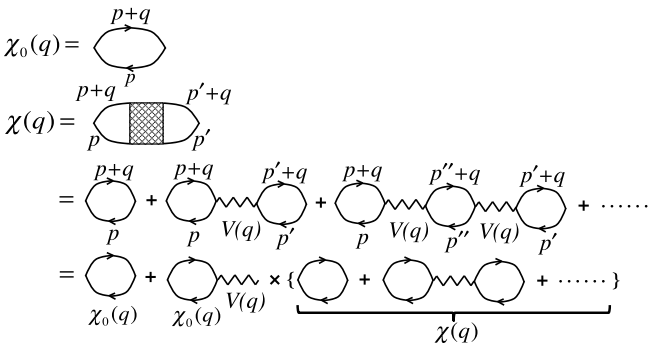

FIG. 6. Feynman diagram expansion of density-density correlation function. χ_0 is the bare response; $\chi(q)$ is the full response function. The wiggly curves denote interaction, and the solid curves with forward and backward pointing arrows represent particles and holes.

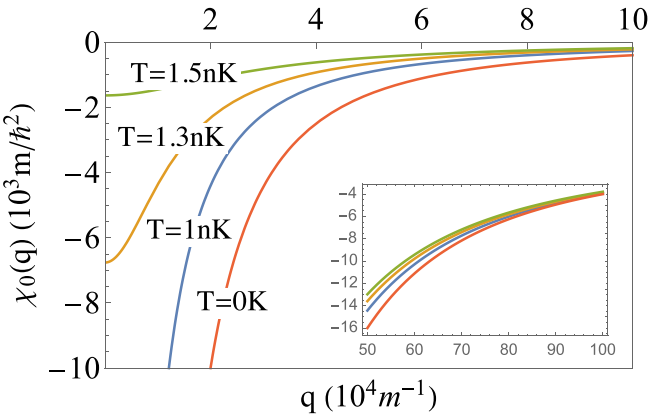

FIG. 7. Bare response function calculated using mass of polar molecule ^{87}Rb ^{133}Cs at density $n = 10^{12}\,\mathrm{m}^{-2}$ at varying temperatures. The inset is the response function at large momentum, showing that the curves asymptotically approach each other.

We thank J. Boronat and G. Baym for useful discussions. We acknowledge funds from Institute for Complex Adaptive Matter. K.F.Q. acknowledges the hospitality of Aspen Center for Physics, where part of the work was done.

APPENDIX A: RPA DIAGRAMMATIC EXPANSION

The diagrammatic expansion of the density-density correlation function $\chi(q)$ in terms of the bare response function χ_0 is shown in Fig. 6.

APPENDIX B: FINITE-TEMPERATURE 2D BOSON BARE BUBBLE

We derive the 2D boson bare bubble at finite temperature with chemical potential μ.

We first shift $f(k \pm q/2)$ to $f(k)$ in Eq. (2) and then integrate over angles to obtain

$$\chi_0(q) = -\frac{2m}{\pi\hbar^2 q}\int_0^{\frac{q}{2}} dkk \frac{1}{e^{\beta\varepsilon_k}e^{-\beta\mu}-1}\frac{1}{\sqrt{q^2-4k^2}}. \quad \text{(B1)}$$

In the $q\lambda_T \ll 1$ limit, $e^{\beta\varepsilon_k} = e^{\frac{(k\lambda_T)^2}{4\pi}} \simeq 1 + O(k\lambda_T)^2$. Integrating out k, we obtain

$$\begin{aligned}\chi_0(q) &\simeq -\frac{2m}{\pi\hbar^2 q}\int_0^{\frac{q}{2}} dkk \frac{1}{e^{-\beta\mu}-1}\frac{1}{\sqrt{q^2-4k^2}} \\ &= -\frac{m}{2\pi\hbar^2}\frac{1}{e^{-\beta\mu}-1}[1+O(q\lambda_T)^2]. \quad \text{(B2)}\end{aligned}$$

In the $q\lambda_T \gg 1$ limit, we obtain

$$\begin{aligned}\chi_0(q) &\simeq -\frac{2m}{\pi\hbar^2 q^2}\int_0^{\infty} dkk \frac{1}{e^{\beta\varepsilon_k}e^{-\beta\mu}-1} \\ &= -\frac{4nm}{\hbar^2 q^2}. \quad \text{(B3)}\end{aligned}$$

Figure 7 shows the bare response function for various temperatures.

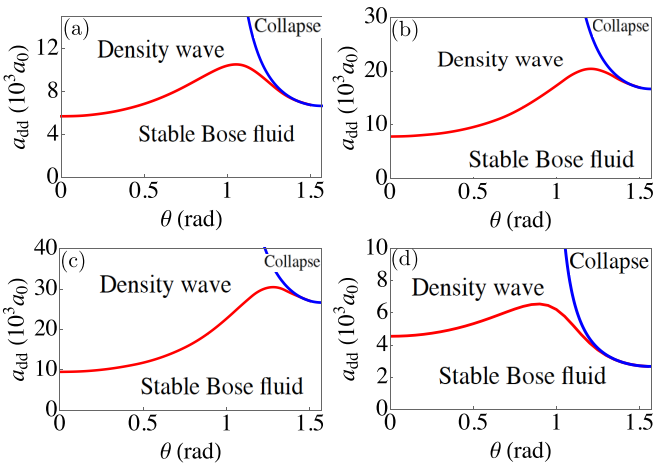

FIG. 8. Effect of adding an additional contact interaction, g. Calculated a_{dd} vs θ phase diagrams of polar molecule ^{87}Rb ^{133}Cs at density $n = 10^{12}\,\mathrm{m}^{-2}$ at $T = 10$ nK. $g = 2\pi\frac{\hbar^2}{2m}a$, with $a = 0, 0.5, 1, -0.2$ for (a), (b), (c), and (d), respectively.

APPENDIX C: ADDITIONAL CONTACT INTERACTION

The plots of the results for the cases of dipolar plus additional repulsive and attractive contact interactions are shown in Fig. 8.

[1] T. Koch, T. Lahaye, J. Metz, B. Frohlich, A. Griesmaier, and T. Pfau, Nat. Phys. **4**, 218 (2008).
[2] K. Aikawa, A. Frisch, M. Mark, S. Baier, A. Rietzler, R. Grimm, and F. Ferlaino, Phys. Rev. Lett. **108**, 210401 (2012).
[3] L. Chomaz, R. M. W. van Bijnen, D. Petter, G. Faraoni, S. Baier, J. H. Becher, M. J. Mark, F. Wächtler, L. Santos, and F. Ferlaino, Nat. Phys. **14**, 442 (2018).
[4] P. K. Molony, P. D. Gregory, Z. Ji, B. Lu, M. P. Köppinger, C. R. Le Sueur, C. L. Blackley, J. M. Hutson, and S. L. Cornish, Phys. Rev. Lett. **113**, 255301 (2014).
[5] T. Takekoshi, L. Reichsöllner, A. Schindewolf, J. M. Hutson, C. R. Le Sueur, O. Dulieu, F. Ferlaino, R. Grimm, and H.-C. Nägerl, Phys. Rev. Lett. **113**, 205301 (2014).
[6] K. Aikawa, D. Akamatsu, J. Kobayashi, M. Ueda, T. Kishimoto, and S. Inouye, New J. Phys. **11**, 055035 (2009).
[7] K. Aikawa, D. Akamatsu, M. Hayashi, K. Oasa, J. Kobayashi, P. Naidon, T. Kishimoto, M. Ueda, and S. Inouye, Phys. Rev. Lett. **105**, 203001 (2010).
[8] A. L. Gaunt, T. F. Schmidutz, I. Gotlibovych, R. P. Smith, and Z. Hadzibabic, Phys. Rev. Lett. **110**, 200406 (2013).
[9] I. Gotlibovych, T. F. Schmidutz, A. L. Gaunt, N. Navon, R. P. Smith, and Z. Hadzibabic, Phys. Rev. A **89**, 061604(R) (2014).
[10] R. Lopes, C. Eigen, A. Barker, K. G. H. Viebahn, M. Robert-de-Saint-Vincent, N. Navon, Z. Hadzibabic, and R. P. Smith, Phys. Rev. Lett. **118**, 210401 (2017).

[11] U. R. Fischer, Phys. Rev. A **73**, 031602(R) (2006).
[12] L. Santos, G. V. Shlyapnikov, and M. Lewenstein, Phys. Rev. Lett. **90**, 250403 (2003).
[13] A. K. Fedorov, I. L. Kurbakov, Y. E. Shchadilova, and Y. E. Lozovik, Phys. Rev. A **90**, 043616 (2014).
[14] Z.-K. Lu, Y. Li, D. S. Petrov, and G. V. Shlyapnikov, Phys. Rev. Lett. **115**, 075303 (2015).
[15] P. Shen and K. Quader, J. Phys. Conf. Ser. **1041**, 012011 (2018).
[16] A. Macia, J. Boronat, and F. Mazzanti, Phys. Rev. A **90**, 061601(R) (2014).
[17] R. Bombin, J. Boronat, and F. Mazzanti, Phys. Rev. Lett. **119**, 250402 (2017).
[18] M. Boninsegni and N. V. Prokof'ev, Rev. Mod. Phys. **84**, 759 (2012).
[19] M. Wenzel, F. Böttcher, T. Langen, I. Ferrier-Barbut, and T. Pfau, Phys. Rev. A **96**, 053630 (2017).
[20] L. Tanzi, E. Lucioni, F. Famà, J. Catani, A. Fioretti, C. Gabbanini, R. N. Bisset, L. Santos, and G. Modugno, Phys. Rev. Lett. **122**, 130405 (2019).
[21] F. Böttcher, J.-N. Schmidt, M. Wenzel, J. Hertkorn, M. Guo, T. Langen, and T. Pfau, Phys. Rev. X **9**, 011051 (2019).
[22] L. Chomaz, D. Petter, P. Ilzhöfer, G. Natale, A. Trautmann, C. Politi, G. Durastante, R. M. W. van Bijnen, A. Patscheider, M. Sohmen, M. J. Mark, and F. Ferlaino, Phys. Rev. X **9**, 021012 (2019).
[23] F. Cinti and M. Boninsegni, J. Low Temp. Phys. **196**, 413 (2019).
[24] R. Bombín, F. Mazzanti, and J. Boronat, Phys. Rev. A **102**, 047302 (2020).
[25] C. Eberlein, S. Giovanazzi, and D. H. J. O'Dell, Phys. Rev. A **71**, 033618 (2005).
[26] K. Sun, C. Wu, and S. Das Sarma, Phys. Rev. B **82**, 075105 (2010).
[27] Y. Yamaguchi, T. Sogo, T. Ito, and T. Miyakawa, Phys. Rev. A **82**, 013643 (2010).
[28] E. J. Mueller and G. Baym, Phys. Rev. A **62**, 053605 (2000).
[29] B. P. van Zyl, R. K. Bhaduri, and J. Sigetich, J. Phys. B: At. Mol. Opt. Phys. **35**, 1251 (2002).
[30] R. N. Bisset, D. Baillie, and P. B. Blakie, Phys. Rev. A **83**, 061602(R) (2011).
[31] For dipolar interaction, the exchange scattering process is independent of momentum q and dominated by small momentum transfers due to Bose statistics. This is thus less important compared with the direct interaction where the momentum transfer is q. We note that for contact interaction, however, both the direct and exchange processes contribute equally, and both need to be taken into account [28].
[32] P. Nozieres, *Theory of Quantum Liquids: Superfluid Bose Liquids* (CRC, Boca Raton, 2018).
[33] C.-K. Chan, C. Wu, W.-C. Lee, and S. Das Sarma, Phys. Rev. A **81**, 023602 (2010).
[34] A. Filinov, N. V. Prokof'ev, and M. Bonitz, Phys. Rev. Lett. **105**, 070401 (2010).
[35] R. Bombín, F. Mazzanti, and J. Boronat, Phys. Rev. A **100**, 063614 (2019).